DOI: https://doi.org/10.15407/pmach2022.01.006

UDC 539.3

DYNAMIC INSTABILITY OF A THREE-LAYER CONICAL SHELL WITH HONEYCOMB STRUCTURE MADE BY ADDITIVE TECHNOLOGIES

Kostiantyn V. Avramov
kvavramov@gmail.com,
ORCID: 0000-0002-8740-693X

Borys V. Uspenskyi
Uspensky.kubes@gmail.com,
ORCID: 0000-0001-6360-7430

Iryna V. Biblik
miles@ipmach.kharkov.ua,
ORCID: 0000-0002-8650-1134

A. Pidhornyi Institute of Mechanical Engineering Problems of NASU
2/10, Pozharskyi str., Kharkiv,
61046, Ukraine

A mathematical model of the dynamic instability of a three-layer conical shells with honeycomb structure made using additive technologies has been obtained. Dynamic instability is recognized as the interaction of the shell with a supersonic gas flow. The middle layer of the structure is a honeycomb that is homogenized into an orthotropic homogeneous medium. The top and bottom layers of the shell are made of carbon fiber. The vibrations of the structure are described by fifteen unknowns. Each layer of the structure is described by five unknowns: three projections of displacements of the layer middle surface and two rotation angles of the normal of the layer middle surface. The high-order shear theory is used to describe the deformation state of the structure. The relation between stresses and strains is expressed by a power expansion in the transverse coordinate up to its cubic terms. To obtain a system of ordinary differential equations describing dynamic instability, the method of given forms is used. To assess the dynamic instability, characteristic indicators are calculated by solving the generalized problem of eigenvalues. The natural vibrations of the structure are studied by the Rayleigh-Ritz method. The minimum natural frequency in the cantilevered shell is observed when the number of waves in the circumferential direction is 6. It is also observed in the shell clamped on both sides when the number of waves in the circumferential direction is 1. The dynamic instability properties of the trivial equilibrium state of the structure are studied using numerical simulation. Shells that are cantilevered and clamped on both sides are analyzed. It is shown that the minimum critical pressure is observed when the number of waves in the circumferential direction is 1. The dependence of the critical pressure on the Mach number and angle of attack is studied. It has been established that with an increase in the Mach number and angle of attack, the critical pressure decreases.

Keywords: *linear dynamic system, three-layer conical shell, characteristic exponents, Mach numbers.*

Introduction

As is known, three-layer composite structures are widely used in aerospace engineering, which is explained by their high strength, rigidity, and low weight. With this in consideration, much effort has been made to study their dynamic properties. Nonlinear vibrations of a viscoelastic composite shell of double curvature with an elastic middle layer and a magnetorheological layer are studied in [1]. Nonlinear vibrations of composite three-layer shells of double curvature with a piezoelectric layer are considered in [2]. To derive the equations of motion, the high-order shear theory and von Karman theory of geometrically nonlinear deformation are used. The nonlinear dynamics of a shallow shell of double curvature with honeycomb structure having a negative Poisson's ratio under the action of an explosion is studied in [3]. Geometrically nonlinear forced vibrations of a cylindrical three-layer shell are modeled in [4], using a high-order shear theory. The article [5] studies the nonlinear dynamics of three-layer cylindrical panels on an elastic foundation under the action of an explosive load. Vibrations of a thin-walled structure of double curvature with honeycomb structure are studied in [6]. To derive the equations of motion, the Hamilton's variational principle is used. In [7], a finite element formulation of the problem is considered taking into account the Green-Lagrange nonlinear deformation.

This paper presents a new mathematical model of the dynamic instability of the three-layer conical shells with honeycomb structure made using additive FDM technologies. The deformation state of each layer is described by five parameters (three projections of the middle surface displacements, two rotation angles of the normal of the layer middle surface). High-order shear theory and geometrically nonlinear deformation are used to describe the stress-strain state of the structure. The properties of dynamic instability of the structure in the supersonic gas flow are numerically investigated.

Problem formulation and main relations

The design of the three-layer conical shell is shown in Fig. 1, a. The middle layer of the shell is ULTEM 9085 FDM honeycomb structure and the top and bottom front sides are made of carbon fiber. One honeycomb cell is shown in Fig. 1, b. Its main geometric parameters are as follows: l_1, l_2, h_c, ψ, where h_c is the honeycomb wall thickness. The dynamic instability of the three-layer conical shells, which arises due to the interaction of the supersonic gas flow with the structure, is considered. It is assumed that the material of both the front layers during deformation and honeycomb structure satisfy Hooke's law.

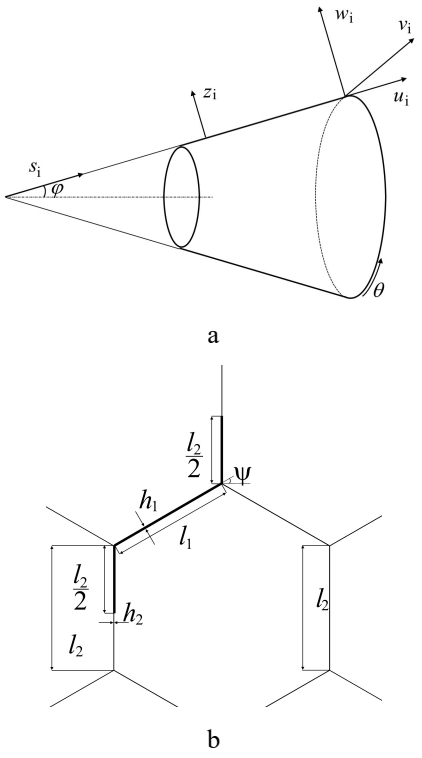

Fig. 1. Design of the conical shell and honeycomb structure

Three curvilinear coordinate systems that will be associated with the middle surfaces of each layer are introduced. The curvilinear coordinates of the top, bottom layers and honeycombs will be denoted by (s_t, θ, z_t), (s_c, θ, z_c), (s_b, θ, z_b), where (s_t, s_c, s_b) – longitudinal coordinates directed along the generatrixes of the median surfaces of the corresponding layer (Fig. 1); θ – circumferential coordinate; (z_t, z_c, z_b) – transverse layer coordinates; s_t, s_c, s_b: $s_t^{(1)}$, $s_c^{(1)}$, $s_b^{(1)}$ – coordinates of the left end side of the conical shell (with smaller radius); $s_t^{(2)}$, $s_c^{(2)}$, $s_b^{(2)}$ – coordinates of the right end side (with larger radius). One longitudinal coordinate ξ for the entire multi-layer construction is introduced and is: $\xi=s_i-s_i^{(1)}$; $i=t, b, c$. The length of the conical shell is denoted by L: $L=s_i^{(2)}-s_i^{(1)}$; $i=t, b, c$. The radii of curvature of the layers middle surfaces are denoted by $R_\theta^{(j)}$; $R_s^{(j)}$; $j=t, b, c$, and Lamé parameters are $A_s^{(j)}$; $A_\theta^{(j)}$. These quantities are defined as follows: $R_\theta^{(j)} = (s_j^{(1)} + \xi)\mathrm{tg}(\varphi)$; $R_s^{(j)} = \infty$; $j=t, c, b$; $A_s^{(j)} = 1$;

$A_\theta^{(j)} = (s_j^{(1)} + \xi)\sin(\varphi)$.

The honeycomb structure is transformed into an equivalent orthotropic layer as a result of its homogenization [8]. In this case, the elements of the stress and strain tensors of the honeycomb layer satisfy Hooke's law:

$$\begin{bmatrix}\sigma_{ss}^{(c)}\\ \sigma_{\theta\theta}^{(c)}\\ \sigma_{zz}^{(c)}\end{bmatrix} = \begin{bmatrix}C_{11} & C_{12} & C_{13}\\ C_{21} & C_{22} & C_{23}\\ C_{31} & C_{32} & C_{33}\end{bmatrix}\begin{bmatrix}\varepsilon_{ss}^{(c)}\\ \varepsilon_{\theta\theta}^{(c)}\\ \varepsilon_{zz}^{(c)}\end{bmatrix};\ \sigma_{\theta z}^{(c)} = 2C_{44}\varepsilon_{\theta z}^{(c)};\ \sigma_{sz}^{(c)} = 2C_{55}\varepsilon_{sz}^{(c)};\ \sigma_{s\theta}^{(c)} = 2C_{66}\varepsilon_{s\theta}^{(c)}.$$

The top and bottom layers of the conical shell are orthotropic. They satisfy Hooke's law:

$$\begin{bmatrix}\sigma_{ss}^{(j)}\\ \sigma_{\theta\theta}^{(j)}\end{bmatrix} = \begin{bmatrix}\overline{C}_{11} & \overline{C}_{12}\\ \overline{C}_{21} & \overline{C}_{22}\end{bmatrix}\begin{bmatrix}\varepsilon_{ss}^{(j)}\\ \varepsilon_{\theta\theta}^{(j)}\end{bmatrix};\ \sigma_{s\theta}^{(j)} = 2\overline{C}_{33}2\varepsilon_{s\theta}^{(j)};\ \sigma_{sz}^{(j)} = 2\overline{C}_{44}\varepsilon_{sz}^{(j)};\ \sigma_{\theta z}^{(j)} = 2\overline{C}_{55}\varepsilon_{\theta z}^{(j)};\ j=b, t.$$

The displacement projections of the top and bottom layers $u_1^{(i)}$, $u_2^{(i)}$, $u_3^{(i)}$ can be presented as follows:

$$u_1^{(i)} = u^{(i)} + z_i\phi_1^{(i)} + z_i^2\psi_1^{(i)};\ u_2^{(i)} = \left(1 + \frac{z_i}{(s_i^{(1)} + \xi)\mathrm{tg}(\varphi)}\right)v^{(i)} + z_i\phi_2^{(i)} + z_i^2\psi_2^{(i)};\ u_3^{(i)} = w^{(i)};\ i=t, b, \quad (1)$$

where $u^{(i)}$, $v^{(i)}$, $w^{(i)}$ are projections of displacements of the middle surfaces points on coordinate axes; $\phi_1^{(i)}$, $\phi_2^{(i)}$ are rotation angles of the normal to the middle surface.

Projections of the middle layer displacements $u_1^{(c)}$, $u_2^{(c)}$, $u_3^{(c)}$ are presented in the form:

$$u_1^{(c)} = u^{(c)} + z_c\phi_1^{(c)} + z_c^2\psi_1^{(c)} + z_c^3\gamma_1^{(c)};\ u_2^{(c)} = \left(1 + \frac{z_c}{(s_c^{(1)} + \xi)\mathrm{tg}(\varphi)}\right)v^{(c)} + z_c\phi_2^{(c)} + z_c^2\psi_2^{(c)} + z_c^3\gamma_2^{(c)};$$

$$u_3^{(c)} = w^{(c)} + z_c w_1^{(c)} + z_c^2 w_2^{(c)}. \quad (2)$$

The designations of relations (1) and (2) coincide. To determine the expansion parameters (1), the following boundary conditions are used:

$$\sigma_{sz}\Big|_{z_t=0,5h_t}=\sigma_{\theta z}\Big|_{z_t=0,5h_t}=0\,;\ \sigma_{sz}\Big|_{z_b=-0,5h_b}=\sigma_{\theta z}\Big|_{z_b=-0,5h_b}=0\,, \tag{3}$$

where h_t, h_b are top and bottom layer thicknesses.

The conditions for the continuity of displacements between layers have the following form:

$$u_i^{(t)}(z_t=-0,5h_t)=u_i^{(c)}(z_c=0,5h_c)\,;\ u_1^{(b)}(z_b=0,5h_b)=u_1^{(c)}(z_c=-0,5h_c)\,;\ i=1,\,2,\,3, \tag{4}$$

where h_c is the middle layer thickness.

Components of expansions (3), (4) $\psi_1^{(t)}$, $\psi_2^{(t)}$, $\psi_1^{(b)}$, $\psi_2^{(b)}$, $\psi_1^{(c)}$, $\gamma_1^{(c)}$, $\psi_2^{(c)}$, $\gamma_2^{(c)}$, $w_1^{(c)}$, $w_2^{(c)}$ are determined from the conditions (3), (4).

The general case of geometrically nonlinear relations describing the deformation of arbitrary shells was published in [9]. These relations are used in expansions (1), (2). Then the relation between deformations and displacements takes the following form:

$$\begin{gathered}\varepsilon_{ss}^{(i)}=\varepsilon_{s,0}^{(i)}+z_ik_{s,0}^{(i)}+z_i^2k_{s,1}^{(i)}+z_i^3k_{s,2}^{(i)}\,;\quad \varepsilon_{\theta\theta}^{(i)}=\varepsilon_{\theta,0}^{(i)}+z_ik_{\theta,0}^{(i)}+z_i^2k_{\theta,1}^{(i)}+z_i^3k_{\theta,2}^{(i)}\,;\\ \varepsilon_{s\theta}^{(i)}=\varepsilon_{s\theta,0}^{(i)}+z_ik_{s\theta,0}^{(i)}+z_i^2k_{s\theta,1}^{(i)}+z_i^3k_{s\theta,2}^{(i)}\,;\quad \varepsilon_{sz}^{(i)}=\varepsilon_{sz,0}^{(i)}+z_ik_{sz,0}^{(i)}+z_i^2k_{sz,1}^{(i)}+z_i^3k_{sz,2}^{(i)}\,;\\ \varepsilon_{\theta z}^{(i)}=\varepsilon_{\theta z,0}^{(i)}+z_ik_{\theta z,0}^{(i)}+z_i^2k_{\theta z,1}^{(i)}+z_i^3k_{\theta z,2}^{(i)}\,;\quad i=t,\,c,\,b;\\ \varepsilon_{zz}^{(c)}=\varepsilon_{z,0}^{(c)}+z_ck_{z,0}^{(c)}\,.\end{gathered} \tag{5}$$

For brevity, the coefficients of these expansions are not given.

The formula by which the potential energy of the shell top and bottom layers is calculated takes the following form:

$$\begin{gathered}U_i=0,5\int\limits_{A_i}(\overline{C}_{11}\varepsilon_{ss}^{(i)2}+\overline{C}_{22}\varepsilon_{\theta\theta}^{(i)2}+2\overline{C}_{12}\varepsilon_{ss}^{(i)}\varepsilon_{\theta\theta}^{(i)}+2\overline{C}_{33}\varepsilon_{\theta z}^{(i)2}+2\overline{C}_{44}\varepsilon_{sz}^{(i)2}+2\overline{C}_{55}\varepsilon_{\theta z}^{(i)2})\times\\ \times\left(1+\frac{z_i}{(s_i^{(1)}+\xi)\mathrm{tg}\varphi}\right)(s_i^{(1)}+\xi)\sin\varphi\,d\xi d\theta dz_i\,;\quad i=t,\,b,\end{gathered} \tag{6}$$

where A_i is the region of the layer middle surface.

Expansions (5) are used to determine potential energy (6) with integration over z_i. As a result, the potential energy is presented as a double integral:

$$U_i=0,5\int\limits_{A_i}\left(\Pi_i^{(0)}+\Pi_i^{(2)}+\Pi_i^{(4)}\right)(s_i^{(1)}+\xi)\sin\varphi\,d\xi d\theta\,;\quad i=t,\,b. \tag{7}$$

The coefficients of expression (7) $\Pi_i^{(0)}$, $\Pi_i^{(2)}$, $\Pi_i^{(4)}$ depend on the expansion coefficients (5). However, for the sake of brevity, these dependences are not given.

The formula for calculating the potential energy of a homogenized middle layer takes the following form:

$$\begin{gathered}U_c=0,5\int\limits_{A_i}(C_{11}\varepsilon_{ss}^{(c)2}+C_{22}\varepsilon_{\theta\theta}^{(c)2}+C_{33}\varepsilon_{zz}^{(c)2}+2C_{12}\varepsilon_{ss}^{(c)}\varepsilon_{\theta\theta}^{(c)}+2C_{13}\varepsilon_{ss}^{(c)}\varepsilon_{zz}^{(c)}+2C_{23}\varepsilon_{\theta\theta}^{(c)}\varepsilon_{zz}^{(c)}+2C_{44}\varepsilon_{\theta z}^{(c)2}+2C_{55}\varepsilon_{sz}^{(c)2}+2C_{66}\varepsilon_{s\theta}^{(c)2})\times\\ \times\left(1+\frac{z_i}{(s_c^{(1)}+\xi)\mathrm{tg}\varphi}\right)(s_c^{(1)}+\xi)\sin\varphi\,d\xi d\theta dz_c\,.\end{gathered} \tag{8}$$

Expansions (5) are used to determine the potential energy (8). Then the potential energy formula (8) is presented in the form (7).

The kinetic energy of each layer separately can be presented as follows:

$$T_i=0,5\int\limits_0^{2\pi s_i^{(2)}}\int\limits_{s_i^{(1)}}^{}\int\limits_{-0,5h_i}^{0,5h_i}\rho_i(\dot{u}_1^{(i)2}+\dot{u}_2^{(i)2}+\dot{u}_3^{(i)2})\left(1+\frac{z_i}{(s_i^{(1)}+\xi)\mathrm{tg}\varphi}\right)(s_i^{(1)}+\xi)\sin\varphi\,d\xi d\theta dz_i\,;\quad i=t,\,c,\,b, \tag{9}$$

where ρ_i is a construction layer material density; $\dot{u}_1^{(i)}=\dfrac{\partial u_1^{(i)}}{\partial t}$.

Expansions (1), (2) are used to find the kinetic energy (9) with integration over z_i. As a result, the following expressions for the kinetic energies are obtained:

$$T_i = 0{,}5\int_0^{2\pi}\int_{s_i^{(1)}}^{s_i^{(2)}} (\Lambda_0^{(i)} + \Lambda_2^{(i)} + \Lambda_4^{(i)})(s_i^{(1)} + \xi)\sin\varphi\, d\xi d\theta\ ;\ i=t,\ c,\ b, \tag{10}$$

where values $\Lambda_0^{(i)}$, $\Lambda_2^{(i)}$, $\Lambda_4^{(i)}$, depend on $\dot{u}^{(i)}$, $\dot{v}^{(i)}$, $\dot{w}^{(i)}$.

The pressure p acting on a conical shell in the supersonic gas flow is described by the piston theory [10]:

$$p = \frac{\gamma p_\infty M^2}{\sqrt{M^2-1}}\left[\frac{\partial w_t}{\partial \xi}\cos\beta + \frac{\partial w_t}{R(\xi)\partial\theta}\sin\beta + \frac{M^2-2}{(M^2-1)Ma_\infty}\frac{\partial w_t}{\partial t} - \frac{w_t}{2R(\xi)\sqrt{M^2-1}}\right], \tag{11}$$

where β is the angle of attack; p_∞ is the flow static pressure; M is the Mach number; γ is the adiabatic index; a_∞ is the sonic speed; $R(\xi) = (s_t^{(1)} + \xi)\sin\varphi$.

To study self-vibrations, the method of given forms is used [11]. In this case, kinematic boundary conditions are taken into account and force boundary conditions are not. If the side of the shell s_i=$s_i^{(1)}$ is clamped, then the kinematic boundary conditions

$$w^{(i)}\Big|_{s_i=s_i^{(1)}} = v^{(i)}\Big|_{s_i=s_i^{(1)}} = u^{(i)}\Big|_{s_i=s_i^{(1)}} = \phi_1^{(i)}\Big|_{s_i=s_i^{(1)}} = \phi_2^{(i)}\Big|_{s_i=s_i^{(1)}} = 0\,.$$

Equations of motion

Let's derive a dynamical system with a finite number of degrees of freedom, which describes the instability of the three-layer conical shell during its interaction with the supersonic gas flow. To do this, the method of given forms is used. Self-vibrations are expanded in terms of natural forms of linear vibrations of the structure

$$w^{(i)} = \sum_{j=1}^{N_w} W_{i,j}(\xi)\left[q_{i,j}(t)\cos(n\theta) + q_{i,j+N_w}(t)\sin(n\theta)\right];$$

$$\phi_1^{(i)} = \sum_{j=1}^{N_{\phi 1}} X_{i,j}(\xi)\left[q_{i,2N_w+j}(t)\cos(n\theta) + q_{i,2N_w+N_{\phi 1}+j}(t)\sin(n\theta)\right];$$

$$\phi_2^{(i)} = \sum_{j=1}^{N_{\phi 2}} Y_{i,j}(\xi)\left[q_{i,2N_w+2N_{\phi 1}+j}(t)\cos(n\theta) + q_{i,2N_w+N_{\phi 1}+N_{\phi 2}+j}(t)\sin(n\theta)\right];$$

$$u^{(i)} = \sum_{j=1}^{N_u} U_{i,j}(\xi)\left[q_{i,2N_w+2N_{\phi 1}+2N_{\phi 2}+j}(t)\cos(n\theta) + q_{i,2N_w+N_{\phi 1}+N_{\phi 2}+N_u+j}(t)\sin(n\theta)\right];$$

$$v^{(i)} = \sum_{j=1}^{N_u} U_{i,j}(\xi)\left[q_{i,2N_w+2N_{\phi 1}+2N_{\phi 2}+2N_u+j}(t)\cos(n\theta) + q_{i,2N_w+N_{\phi 1}+N_{\phi 2}+N_u+N_v+j}(t)\sin(n\theta)\right];\ i=t,\ c,\ b, \tag{12}$$

where **q** is the vector of generalized coordinates;

$$\mathbf{q} = [q_{1,1},\ldots,q_{1,2N_w+2N_{\phi 1}+2N_{\phi 2}+2N_u+2N_v},\ldots,q_{3,1},\ldots,q_{3,2N_w+2N_{\phi 1}+2N_{\phi 2}+2N_u+2N_v}] = [q_1,\ldots,q_{N_*}];$$

N_* is the number of the structure degrees of freedom; $W_{i,j}(\xi)$, $X_{i,j}(\xi)$, $Y_{i,j}(\xi)$, $U_{i,j}(\xi)$, $V_{i,j}(\xi)$ – eigenfrequency of the structure.

Expansion (12) is introduced into (7), (8) and the required integration is performed. As a result, the formula for calculating the potential energy is obtained in the form of a polynomial with respect to generalized coordinates: $U_\Sigma = \Lambda_2(\mathbf{q})$, where $\Lambda_2(\mathbf{q})$ is the sum of polynomials of degree 2. Expression (12) is used in (9), (10) and integration is performed. The kinetic energy takes the following form: $T_\Sigma = \sigma_2(\dot{\mathbf{q}})$, $\sigma_2(\dot{\mathbf{q}})$ is the quadratic polynomial in generalized velocities. The generalized forces corresponding to the aerodynamic pressure are found (11). Then the virtual work is presented as:

$$\delta A = -\int_0^{2\pi} \int_{s_t^{(1)}}^{s_t^{(2)}} p\delta w^{(t)} (s_t^{(1)} + \xi) \sin\varphi \, d\xi d\theta = \sum_{j=1}^{N^{(w)}} Q_{1,j} \delta q_j ,$$

where $\delta w^{(i)}$ is the virtual displacement; Q_j is the generalized force.

Expression (12) is used in (11). Then we present the generalized forces in the following form:

$$Q_{1,j_1} = \sum_{j=1}^{2N_w} G_{j_1,j}^{(1)} q_{1,j} + \sum_{j=1}^{N_w} \Gamma_{j_1,j}^{(1)} \dot{q}_{1,j} ; \quad Q_{1,j_1+N_w} = \sum_{j=1}^{2N_w} G_{j_1+N_w,j}^{(1)} q_{1,j} + \sum_{j=1}^{N_w} \Gamma_{j_1+N_w,j}^{(1)} \dot{q}_{1,j+N_w} ; j_1=1, \ldots, N_w.$$

The Lagrange equations of the structure motion take the following form:

$$\mathbf{M}\ddot{\mathbf{q}} + \mathbf{K}\mathbf{q} = \mathbf{G}\mathbf{q} + \mathbf{\Gamma}\dot{\mathbf{q}} , \tag{13}$$

where $\mathbf{G}$ is a aerodynamic stiffness matrix; $\mathbf{\Gamma}$ is a aerodynamic damping matrix.

As it can be seen from the results of numerical simulation of system (13), most of the elements of the matrix $\mathbf{M}$ are close to zero. This is due to the fact that the top and bottom layers are very thin, and the middle one has low density. To describe this fact, the main matrices and vectors of system (13) are presented as

$$\mathbf{M} = \begin{bmatrix} \mathbf{M_{11}} & \mathbf{M_{12}} \\ \mathbf{M_{21}} & \mathbf{M_{22}} \end{bmatrix}; \ \mathbf{K} = \begin{bmatrix} \mathbf{K_{11}} & \mathbf{K_{12}} \\ \mathbf{K_{21}} & \mathbf{K_{22}} \end{bmatrix}; \ \mathbf{q} = [\mathbf{q}_1, \mathbf{q}_2]^{\mathrm{T}} .$$

Then the next elements of the matrix, which are very small, can be considered zero: $\mathbf{M}_{21}\equiv 0$; $\mathbf{M}_{22}\equiv 0$; $\mathbf{M}_{12}\equiv 0$.

Equation (13) can be presented as

$$\mathbf{M}_{11}\ddot{\mathbf{q}}_1 + \overline{\mathbf{K}}_{11}\mathbf{q}_1 = \mathbf{G}\mathbf{q}_1 + \mathbf{\Gamma}\dot{\mathbf{q}}_1 , \tag{14}$$

where $\overline{\mathbf{K}}_{11} = \mathbf{K}_{11} - \mathbf{K}_{12}\mathbf{K}_{22}^{-1}\mathbf{K}_{21}$.

The stability of the trivial equilibrium state $q_1\equiv 0$ of the dynamical system (14) is studied. The obtained linear dynamical system has the solution $(\mathbf{q}_1, \dot{\mathbf{q}}_1) \equiv (\mathbf{q}_1, \mathbf{v}) = P_* \exp(\lambda t)$, where λ is the characteristic exponent.

This solution is introduced into the dynamical system (14). Then the generalized eigenvalue problem is obtained:

$$\mathbf{R}\lambda\mathbf{P}_* = \Im\mathbf{P}_* ,$$

where $\mathbf{R} = \begin{bmatrix} \mathbf{E} & \mathbf{0} \\ \mathbf{0} & \mathbf{M_{11}} \end{bmatrix}$; $\Im = \begin{bmatrix} \mathbf{0} & \mathbf{E} \\ \mathbf{G} - \mathbf{K_{11}} & \mathbf{\Gamma} \end{bmatrix}$; $\mathbf{E}$ is the identity matrix.

The values of λ determine the stability of the trivial equilibrium state.

Numerical analysis

The eigenfrequencies of the three-layer conical shell are studied. The shell clamped on both sides and the cantilevered structure are considered. The honeycomb structure is made using FDM technology from ULTEM 9085 material. The mechanical parameters of ULTEM 9085 material were determined experimentally. The results of these experiments are presented in the article [12]. A finite element modeling of the honeycomb structure was carried out to determine the mechanical properties of an orthotropic homogenized medium. In this paper, this approach won't be considered. Instead, the results of mechanical properties modeling will be presented. The geometric parameters of the honeycomb structure (Fig. 1, b) were taken as follows: l_1=6.1054 mm; l_2=3.0527 mm; θ=60 °; l_c=10 mm; $\overline{h}_c$=0.4 mm, where $\overline{h}_c$ is the wall thickness of the honeycomb structure; l_c is the height of the honeycomb structure. Engineering constants of homogenized honeycomb structure take the following numerical values:

$$E_{11}=2.91 \text{ MPa}; E_{22}=2.91 \text{ MPa}; E_{33}=215.10 \text{ MPa}; \nu_{12}=0.971; \nu_{23}=0.0051; \nu_{13}=0.0042;$$
$$G_{12}=1.118 \text{ MPa}; G_{23}=39.1 \text{ MPa}; G_{13}=39.1 \text{ MPa}; \rho_c=253.189 \text{ kg/m}^3. \tag{15}$$

The engineering constants of the top and bottom layers are:

$$E_x=160\cdot 10^9 \text{ Pa}; E_y=160\cdot 10^9 \text{ Pa}; \nu_{xy}=0.32; \nu_{yx}=0.0136; G_{xy}=800\cdot 10^9 \text{ Pa};$$
$$G_{xz}=G_{yz}=4\cdot 10^9 \text{ Pa}; \rho_t=\rho_b=1400 \text{ kg/m}^3. \tag{16}$$

The conical shell has the following values of the structure geometric parameters:

$$\varphi=\pi/12; s_t^{(1)}=2.354 \text{ m}; s_c^{(1)}=2.33 \text{ m}; s_b^{(1)}=2.313 \text{ m}; h_t=h_b=10^{-3} \text{ m}; h_c=10^{-2} \text{ m}. \tag{17}$$

The first ten natural vibration frequencies of this structure are given in Table 1 in ascending order of natural frequencies. The second column shows the dimension of the generalized eigenvalue problem for calculation of frequencies and vibration shapes. The third column shows the natural frequencies obtained by the Rayleigh-Ritz method. The fourth column shows natural frequencies obtained in the ANSYS software package. The natural frequencies spectrum is extremely dense. So, there are ten natural frequencies observed in the range $\omega \in [411.83; 478.42]$ Hz.

The dependence of the first natural frequency on the number of waves in the circumferential direction is shown in Fig. 2 with a solid line. We emphasize that the minimum natural frequency is observed at n=1. In isotropic shells, the first natural frequency is observed at a much larger number of n.

The linear vibrations of the cantilevered conical shell are investigated. The side with a larger radius (Fig. 1) is clamped, while the side with a smaller radius is free. The geometric dimensions of the three-layer shell have the form (17). The mechanical characteristics of the top and bottom layers have the form (16), and the mechanical characteristics of the middle layer have the form (15).

Table 1. Natural vibration frequencies

n	N_*	ω, Hz	ω_{FEM}, Hz	δ
1	270	411.83	421.98	0.024
2	240	430.10	438.45	0.019
3	240	448.56	455.76	0.015
8	270	450.22	460.61	0.022
7	270	451.41	462.27	0.023
6	270	457.54	467.82	0.022
9	270	458.46	466.99	0.018
4	240	460.24	467.50	0.015
5	240	462.71	471.14	0.018
10	240	478.42	482.81	0.0091

Table 2. Results of calculation of the cantilevered shell natural vibration frequencies

n	N_*	ω, Hz	ω_{FEM}, Hz	δ
1	210	409.46	417.15	0.018
2	210	409.58	409.90	$7.8 \cdot 10^{-4}$
3	210	365.95	353.16	0.036
4	210	307.81	292.54	0.050
5	210	271.49	265.06	0.020
6	210	262.10	264.29	0.006
7	210	274.41	280.20	0.020
8	210	302.77	307.97	0.016
9	210	342.96	345.00	0.006
10	210	391.95	389.58	0.006

The results of calculating the natural vibration frequencies are given in Table 2. Designations of the columns of the Table 1 and Table 2 are the same. As follows from Table 2, the natural frequencies obtained by the two methods are close. The dependence of the first natural frequencies on n is shown in Fig. 2 by dotted line. So, the minimum natural frequency is observed at n=6. It's better to remind that the minimum natural vibration frequency of the clamped shell is observed at n=1.

The linear vibrations of the cantilevered conical shell are qualitatively different from the vibrations of the conical shell clamped on both sides, which follows from the eigenfrequency of the cantilevered shell. The free edge of the cantilevered shell makes intense vibrations. In the shell clamped on both sides, this edge is at rest.

The dynamic instability of the conical shell clamped on both sides is studied. The first ten natural frequencies of its vibrations are given in Table 1. In expansions (12), the following number of terms was chosen $N_w = N_{\phi_1} = N_{\phi_2} = N_u = N_v$. When calculating the regions of dynamic instability, N_w were taken equal to 2; 3; 4. To calculate the dynamic instability of a trivial equilibrium state, the characteristic exponents were determined from the eigenvalues problem.

Fig. 3 shows the boundaries of the region of the shell dynamic instability on the plane of parameters ($p_\infty^{(cr)}$, n), obtained for two values of the Mach numbers M=1.5 and M=5 and for the number of terms in expansion (12) N_w=3. The minimum value of n at which buckling occurs corresponds to n=1. It should be emphasized that critical pressures are observed in isotropic shells at a much larger number of n. The parameters at which there is a loss of stability are called critical. So, with an increase in the Mach number M, the value of the critical pressure decreases.

The effect of the angle of attack on the critical pressure $p_\infty^{(cr)}$ was studied. For this, the analysis of dynamic instability was carried out for different values of the angle β and for one value of the number of waves in the circumferential direction n=1. The results of such analysis are shown in Fig. 4 (solid line). So, as the angle β increases, the value of the critical pressure increases.

The dynamic instability of a cantilevered truncated conical shell was studied. The natural vibration frequencies of such shell are given in Table 2. The boundaries of the region of dynamic instability on the

plane of parameters ($p_\infty^{(cr)}$, n) are shown in Fig. 5. The solid line in this figure shows the boundary of the region of dynamic instability at M=1.5, and the dotted line shows the boundary of the region at M=5. Thus, as the Mach number increases, the value of $p_\infty^{(cr)}$ decreases.

As follows from the calculation results, the minimum critical pressure is observed at n=1. The dependence of the critical pressure $p_\infty^{(cr)}$ at n=1 on the angle of attack β was studied. The results of such calculations are shown by the dotted line in Fig. 4. As the angle β increases, the critical pressure increases.

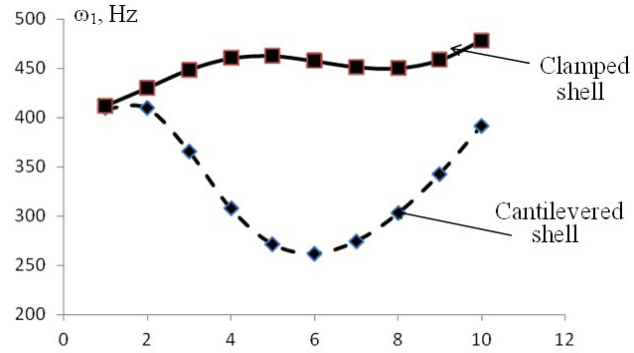

Fig. 2. Dependence of the first natural frequency ω_1 on the number of waves in the circumferential direction n

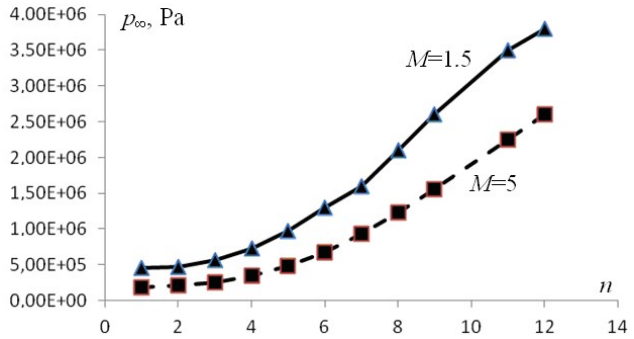

Fig. 3. Areas of dynamic instability of the structure trivial equilibrium

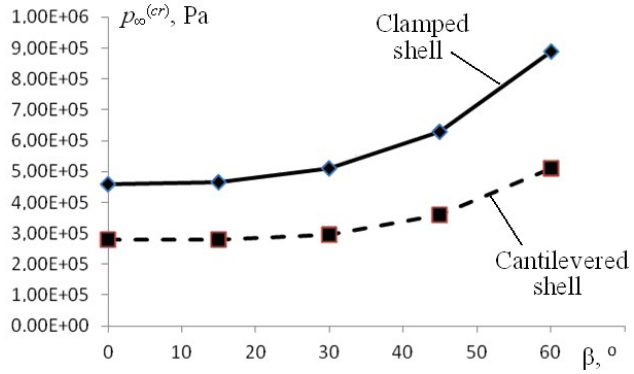

Fig. 4. Dependence of critical pressure on the angle of attack

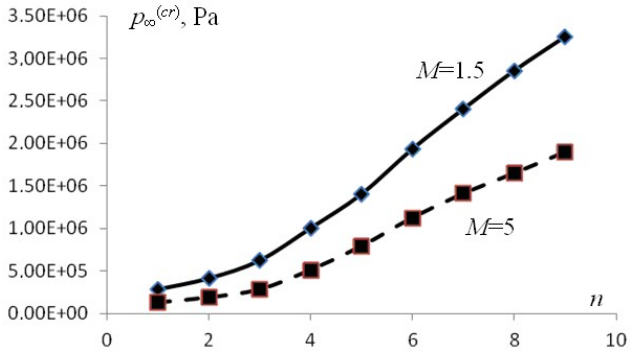

Fig. 5. The boundary of the region of dynamic instability for the cantilevered shell

Conclusion

A mathematical model of the dynamic instability of the conical shell with honeycomb structure made using additive technologies has been developed. The deformation behavior of each layer is described by five parameters (three projections of displacements of the layer middle surface and two rotation angles of the normal to the middle surface). High-order shear theory is used to describe the stress state, and the method of given forms is used to obtain a dynamic instability model.

Using the Rayleigh-Ritz method, the linear vibrations of the cantilevered and conical shell clamped on both sides are investigated. It has been numerically established that the minimum natural frequency for vibrations of the shell clamped on both sides is observed when the number of waves in the circumferential direction is 1, and for vibrations of the cantilevered shell, it is observed when the number of waves in the circumferential direction is 6.

For all boundaries of the region of dynamic instability of the clamped and cantilevered three-layer shell, the minimum value of the critical pressure is observed when the number of waves in the circumferential direction is n=1. As the Mach number M increases, the value of the critical pressure decreases. In the cantilevered conical shell, the critical pressure is less than in the shell clamped on both sides.

Financing

The study was funded by the National Research Foundation of Ukraine (grant 128/02/2020).

References

1. Karimiasl, M. & Ebrahimi, F. (2019). Large amplitude vibration of visco-elastically damped multiscale composite doubly curved sandwich shell with flexible core and MR layers. *Thin-Walled Structures*, vol. 144, paper ID 106128. https://doi.org/10.1016/j.tws.2019.04.020.
2. Karimiasla, M., Ebrahimia, F., & Maheshb, V. (2019). Nonlinear forced vibration of smart multiscale sandwich composite doubly curved porous shell. *Thin-Walled Structures*, vol. 143, paper ID 106152. https://doi.org/10.1016/j.tws.2019.04.044.
3. Cong, P. H., Khanh, N. D., Khoa, N. D., & Duc, N. D. (2018). New approach to investigate nonlinear dynamic response of sandwich auxetic double curves shallow shells using TSDT. *Composite Structures*, vol. 185, pp. 455–465. https://doi.org/10.1016/j.compstruct.2017.11.047.
4. Yadav, A., Amabili, M., Panda, S. K., Dey, T., & Kumar, R. (2021). Forced nonlinear vibrations of circular cylindrical sandwich shells with cellular core using higher-order shear and thickness deformation theory. *Journal of Sound and Vibration*, vol. 510, paper ID 116283. https://doi.org/10.1016/j.jsv.2021.116283.
5. Van Quyen, N., Thanh, N. V., Quan, T. Q., & Duc, N. D. (2021). Nonlinear forced vibration of sandwich cylindrical panel with negative Poisson's ratio auxetic honeycombs core and CNTRC face sheets. *Thin-Walled Structures*, vol. 162, paper ID 107571. https://doi.org/10.1016/j.tws.2021.107571.
6. Zhang, Y. & Li, Y. (2019). Nonlinear dynamic analysis of a double curvature honeycomb sandwich shell with simply supported boundaries by the homotopy analysis method. *Composite Structures*, vol. 221, paper ID 110884. https://doi.org/10.1016/j.compstruct.2019.04.056.
7. Naidu, N. V. S. & Sinha, P. K. (2007). Nonlinear free vibration analysis of laminated composite shells in hygrothermal environments. *Composite Structures*, vol. 77, iss. 4, pp. 475–483. https://doi.org/10.1016/j.compstruct.2005.08.002.
8. Catapano, A. & Montemurro, M. (2014). A multi-scale approach for the optimum design of sandwich plates with honeycomb core. Part I: homogenisation of core properties. *Composite Structure*, vol. 118, pp. 664–676. https://doi.org/10.1016/j.compstruct.2014.07.057.
9. Amabili, M. (2018). Nonlinear mechanics of shells and plates in composite, soft and biological materials. United Kingdom, Cambridge: Cambridge University Press, 568 p. https://doi.org/10.1017/9781316422892.
10. Meirovitch, L. (2001). Fundamentals of vibrations. New York: Mc Graw Hill Press, 806 p. https://doi.org/10.1115/1.1421112.
11. Amabili, M. (2015). Non-linearities in rotation and thickness deformation in a new third-order thickness deformation theory for static and dynamic analysis of isotropic and laminated doubly curved shells. *International Journal of Non-Linear Mechanics*, vol. 69, pp. 109–128. https://doi.org/10.1016/j.ijnonlinmec.2014.11.026.
12. Derevianko, I., Avramov, K., Uspenskyi, B., & Salenko, A. (2021). *Eksperymentalnyi analiz mekhanichnykh kharakterystyk detalei raket-nosiiv, vyhotovlenykh za dopomohoiu FDM adytyvnykh tekhnolohii* [Experimental analysis of mechanical characteristics of parts of launch vehicles manufactured using FDM additive technologies]. *Tekhnichna mekhanika – Technical Mechanics*, iss. 1, pp. 92–100 (in Ukrainian). https://doi.org/10.15407/itm2021.01.092.

Received 11 January 2022

Динамічна нестійкість тришарової конічної оболонки із стільниковим заповнювачем, виготовленим адитивними технологіями

К. В. Аврамов, Б. В. Успенський, І. В. Біблік

Інститут проблем машинобудування ім. А. М. Підгорного НАН України,
61046, Україна, м. Харків, вул. Пожарського, 2/10

Отримано математичну модель динамічної нестійкості тришарових конічних оболонок із стільниковим заповнювачем, виготовленим за допомогою адитивних технологій. Динамічна нестійкість викликана взаємодією оболонки з надзвуковим газовим потоком. Середній шар конструкції є стільниковим заповнювачем, який гомогенізується в ортотропне однорідне середовище. Верхній та нижній шари оболонки виготовляються з вуглепластику. Коливання конструкції описуються п'ятнадцятьма невідомими, а кожен шар конструкції – п'ятьма невідомими: трьома проєкціями переміщень серединної поверхні шару і двома кутами повороту нормалі серединної поверхні шару. Для опису деформаційного стану конструкції використовується зсувна теорія високого порядку. Зв'язок між напруженнями і деформаціями виражається ступеневим розкладанням за попе-

речною координатою аж до її кубічних ступенів. Для отримання системи звичайних диференціальних рівнянь, що описують динамічну нестійкість, використовується метод заданих форм. Для оцінки динамічної нестійкості розраховуються характерні показники із рішення узагальненої проблеми власних значень. Досліджуються власні коливання конструкції методом Релея-Рітца. У консольній оболонці мінімальна власна частота спостерігається при числі хвиль в обводовому напрямку, що дорівнює 6, а в защемленій з двох сторін оболонці мінімальна власна частота – при числі хвиль в обводовому напрямку, що дорівнює 1. За допомогою чисельного моделювання досліджуються властивості динамічної нестійкості тривіального стану рівноваги конструкції. Аналізуються консольні та защемлені з обох боків оболонки. Показано, що мінімальний критичний тиск спостерігається при числі хвиль в обводовому напрямку, що дорівнює 1. Досліджується залежність критичного тиску від числа Маха й кута атаки. Встановлено, що при збільшенні числа Маха і кута атаки критичний тиск падає.

Ключові слова: *лінійна динамічна система, тришарова конічна оболонка, характеристичні показники, числа Маха.*

Література

1. Karimiasl M., Ebrahimi F. Large amplitude vibration of viscoelastically damped multiscale composite doubly curved sandwich shell with flexible core and MR layers. *Thin-Walled Structures*. 2019. Vol. 144. Paper ID 106128. https://doi.org/10.1016/j.tws.2019.04.020.
2. Karimiasla M., Ebrahimia F., Maheshb V. Nonlinear forced vibration of smart multiscale sandwich composite doubly curved porous shell. *Thin-Walled Structures*. 2019. Vol. 143. Paper ID 106152. https://doi.org/10.1016/j.tws.2019.04.044.
3. Cong P. H., Khanh N. D., Khoa N. D., Duc N. D. New approach to investigate nonlinear dynamic response of sandwich auxetic double curves shallow shells using TSDT. *Composite Structures*. 2018. Vol. 185. P. 455–465. https://doi.org/10.1016/j.compstruct.2017.11.047.
4. Yadav A., Amabili M., Panda S. K., Dey T., Kumar R. Forced nonlinear vibrations of circular cylindrical sandwich shells with cellular core using higher-order shear and thickness deformation theory. *Journal of Sound and Vibration*. 2021. Vol. 510. Paper ID 116283. https://doi.org/10.1016/j.jsv.2021.116283.
5. Van Quyen N., Thanh N. V., Quan T. Q., Duc N. D. Nonlinear forced vibration of sandwich cylindrical panel with negative Poisson's ratio auxetic honeycombs core and CNTRC face sheets. *Thin-Walled Structures*. 2021. Vol. 162. Paper ID 107571. https://doi.org/10.1016/j.tws.2021.107571.
6. Zhang Y., Li Y. Nonlinear dynamic analysis of a double curvature honeycomb sandwich shell with simply supported boundaries by the homotopy analysis method. *Composite Structures*. 2019. Vol. 221. Paper ID 110884. https://doi.org/10.1016/j.compstruct.2019.04.056.
7. Naidu N. V. S., Sinha P. K. Nonlinear free vibration analysis of laminated composite shells in hygrothermal environments. *Composite Structures*. 2007. Vol. 77. Iss. 4. P. 475–483. https://doi.org/10.1016/j.compstruct.2005.08.002.
8. Catapano A., Montemurro M. A multi-scale approach for the optimum design of sandwich plates with honeycomb core. Part I: homogenisation of core properties. *Composite Structure.* 2014. Vol. 118. P. 664–676. https://doi.org/10.1016/j.compstruct.2014.07.057.
9. Amabili M. Nonlinear mechanics of shells and plates in composite, soft and biological materials. United Kingdom, Cambridge: Cambridge University Press, 2018. 568 p. https://doi.org/10.1017/9781316422892.
10. Meirovitch L. Fundamentals of vibrations. New York: Mc Graw Hill Press, 2001. 806 p. https://doi.org/10.1115/1.1421112.
11. Amabili M. Non-linearities in rotation and thickness deformation in a new third-order thickness deformation theory for static and dynamic analysis of isotropic and laminated doubly curved shells. *International Journal of Non-Linear Mechanics*. 2015. Vol. 69. P. 109–128. https://doi.org/10.1016/j.ijnonlinmec.2014.11.026.
12. Деревянко І., Аврамов К., Успенський Б., Саленко О. Експериментальний аналіз механічних характеристик деталей ракет-носіїв, виготовлених за допомогою FDM адитивних технології. *Технічна механіка*. 2021. Вип. 1. С. 92–100. https://doi.org/10.15407/itm2021.01.092.